

Vedran Mrzljak  
Igor Poljak  
Jasna Prpić-Oršić



<http://dx.doi.org/10.21278/brod70105>

ISSN 0007-215X  
eISSN 1845-5859

## EXERGY ANALYSIS OF THE MAIN PROPULSION STEAM TURBINE FROM MARINE PROPULSION PLANT

UDC 629.5.016:629.5.03

Original scientific paper

### Summary

The paper presents exergy analysis of main propulsion steam turbine from LNG carrier steam propulsion plant. Measurement data required for turbine exergy analysis were obtained during the LNG carrier exploitation at three different turbine loads. Turbine cumulative exergy destruction and exergy efficiency are directly proportional - they increase during the increase in propulsion propeller speed (steam turbine load). Cumulative exergy destruction and exergy efficiency amounts 2041 kW and 66.01 % at the lowest (41.78 rpm), up to the 5923 kW and 80.72 % at the highest (83.00 rpm) propulsion propeller speed. Increase in propulsion propeller speed resulted with an increase in analyzed turbine developed power from 3964 kW at 41.78 rpm to 24805 kW at 83.00 rpm. Analyzed turbine lost power at the highest propulsion propeller speed is the highest and amounts 3339 kW. Steam content at the main propulsion turbine outlet decreases during the increase in propulsion propeller speed. Exergy flow streams can vary considerably, even for a small difference in propulsion propeller speed. Steam turbine in land-based power plant (high power steam turbine) or in marine steam plant (low power steam turbine) is not the component which exergy destruction or exergy efficiency is significantly influenced by the ambient temperature change. A detail analysis of main propulsion steam turbine from the marine steam power plant at several loads is hard to find in the scientific and professional literature.

*Key words:* marine steam turbine; exergy analysis; propulsion; marine steam plant

### 1. Introduction

In ship propulsion nowadays, diesel engines in general (mostly slow speed diesel engines) have a leading role [1,2], due to several significant advantages. The wide presence of diesel engines in ship propulsion enabled the development of different numerical models for investigation of their operating parameters [3] and for optimization of their processes [4].

Steam propulsion, in general, is only slightly present on ships, but it is still the dominant type of propulsion for LNG (Liquefied Natural Gas) carriers [5] due to the specificity of their operation and the transported cargo. Any steam system is usually very complex because it is assembled from a large number of components [6]. The majority of marine steam propulsion

plant components are the same as components in conventional land-based steam power plants, but their operation principle is much more dynamic. Usually, the marine steam propulsion plant consists of two steam generators [7] due to safety operation and two parallel operating turbo-generators [8] to ensure electricity supply at any time. Propulsion propeller (or more of them) drive is ensured with main propulsion turbine [9]. Steam after expansion in turbo-generators and main propulsion turbine goes to the main condenser [10] on liquefaction.

On water return channel to steam generators there are several devices which provide water heating. The first of such devices is evaporator (fresh water generator) [11], the steam marine plant component which is not required in land-based steam plants. After evaporator is usually located sealing steam condenser [12] and two or more feed water heaters [13,14]. Between feed water heaters is located deaerator [15,16] with its dual function - feed water heating and removal of gaseous components from feed water to reduce corrosion. On water return channel are also mounted hot well [17] for collecting all the condensate from the system and desuperheater. Desuperheater is a heat exchanger which is used for steam cooling and preparation for the purpose of heating the cargo and all auxiliary systems [18]. General marine steam propulsion plant scheme of one conventional LNG carrier can be found in [8].

At this moment, new systems for LNG carrier propulsion, which are at least partially based on steam turbines, are under the development [19]. One of the main goals of such propulsion systems is to reduce greenhouse gas emissions at the lowest possible level [20,21,22]. For such complex marine propulsion systems is necessary to provide the economic and profitability analysis [23] as well as operational risk assessment [24] in order to minimize possible harmful consequences.

This paper presents a complete exergy analysis and exergy flow analysis of main propulsion steam turbine from LNG carrier steam propulsion plant. Analyzed turbine has two cylinders (high pressure and low pressure cylinder) and three steam subtractions. Measurement data required for main propulsion turbine exergy analysis were obtained during the LNG carrier exploitation at three different turbine loads (low load - 41.78 rpm, middle load - 74.59 rpm and high load - 83.00 rpm).

The main propulsion steam turbine is analyzed during the harbour leaving until reaching the cruising speed. Therefore, low turbine load (41.78 rpm) represents the beginning of ship acceleration; middle load (74.59 rpm) is a turbine load during ship acceleration and high turbine load at 83.00 rpm is turbine load at the ship cruising speed. Turbine high load (load at the ship cruising speed) usually amounts around 85 % of turbine maximum (full) load because on such turbine load specific fuel consumption is the lowest. In this particular case, the main turbine developed power at high load (83.00 rpm) amounts 84.3 % of maximum turbine power.

Energy and exergy analysis are widely used methods for the investigation of entire steam power plants or its components [8,16]. Equally, such analyses can be used for the investigation of entire ship energy systems – examples can be found in [25] for chemical tanker or in [26] for a cruise ship. Those methods are black-box methods because such analyses do not require knowledge of any component inner structure - the relevant are only energy and exergy inputs and outputs of the component to obtain its efficiency and losses.

Any steam turbine energy analysis gives as a result comparison of how much real (polytropic) steam expansion process deviates from the ideal (isentropic) steam expansion process throughout the turbine. The comparison of these two steam expansion process allows calculation of turbine real and ideal power, after which is calculated turbine energy losses and energy efficiencies. So, the baseline of any steam turbine energy analysis is comparison of real and ideal steam expansion processes, as presented for marine turbo-generators in [8]. Energy analysis does not take into account the ambient conditions in which turbine operate.

Exergy analysis of the main propulsion steam turbine at different loads will present a change in turbine exergy efficiencies and losses during the load increase - to evaluate the current turbine operation and identify possible problems. Analysis of exergy flows and steam mass flows throughout the main propulsion turbine at different loads can be used as a baseline for turbine (and entire power plant) optimization. Steam content calculation at the main turbine outlet is commonly used for better protection of turbine blades and for increasing a period between maintenance. Exergy analysis, unlike energy analysis, takes into account the conditions of the ambient in which turbine operates what allows analysis of the main propulsion steam turbine exergy efficiencies and losses at different ambient temperatures. At the end - calculated turbine exergy destruction divided by turbine developed power at any load (specific turbine exergy destruction) can be used for direct comparison of main marine propulsion steam turbine with any other steam turbine.

## 2. Steam turbine exergy analysis

### 2.1 General equations for exergy analysis

Mass balance for a standard volume in steady state disregarding potential and kinetic energy can be defined according to [27,28] with an equation:

$$\sum \dot{m}_{IN} = \sum \dot{m}_{OUT} \quad (1)$$

Exergy analysis of any steam plant component is based on the second law of thermodynamics [8,29]. The exergy balance equation for a standard volume (control volume) in steady state is [30,31]:

$$\dot{X}_{heat} - P = \sum \dot{m}_{OUT} \cdot \varepsilon_{OUT} - \sum \dot{m}_{IN} \cdot \varepsilon_{IN} + \dot{E}_{ex,D} \quad (2)$$

where the net exergy transfer by heat ( $\dot{X}_{heat}$ ) at the temperature  $T$  is defined as [32,33]:

$$\dot{X}_{heat} = \sum (1 - \frac{T_0}{T}) \cdot \dot{Q} \quad (3)$$

Specific exergy was defined according to [34,35]:

$$\varepsilon = (h - h_0) - T_0 \cdot (s - s_0) \quad (4)$$

The total exergy of any fluid stream (exergy power) is defined according to [36,37]:

$$\dot{E}_{ex} = \dot{m} \cdot \varepsilon = \dot{m} \cdot [(h - h_0) - T_0 \cdot (s - s_0)] \quad (5)$$

Exergy efficiency is also called second law efficiency or effectiveness [29,38]. In general, it can be defined by using an equation:

$$\eta_{ex} = \frac{\text{Exergy output}}{\text{Exergy input}} \quad (6)$$

### 2.2 Main steam propulsion turbine exergy analysis

Analyzed main steam propulsion turbine is mounted in the steam propulsion power plant of commercial LNG carrier. Main characteristics and specifications of the LNG carrier, on which the main propulsion turbine is mounted, are presented in Table 1:

**Table 1** Main characteristics and specifications of the LNG carrier

Gross tonnage	100450 tons
Dead weight tonnage	84812 tons
Overall length	288 m
Max breadth	44 m
Design draft	9.3 m
Steam generators	2 x Mitsubishi MB-4E-KS
Main propulsion turbine	Mitsubishi MS40-2 (max. power 29420 kW)
Turbo-generators	2 x Shinko RGA 92-2 (max. power 3850 kW each)

Main propulsion turbine consists of two cylinders: high pressure (HP) and low pressure (LP) cylinders, Fig. 1. The HP cylinder consists of eight stages (one Curtis and seven Rateau stages - all for ahead drive) while the LP cylinder consists of ten stages (eight Rateau stages for ahead drive and two Curtis stages for astern drive). At the main turbine, Fig. 1, can be seen three steam subtractions – first from HP cylinder, second between HP and LP cylinder and third from the LP cylinder. Steam subtraction mass flows to each steam plant component were regulated by using electronically driven valves from the main engine room control electronic system [39].

At Fig. 1 can also be seen steam stream flow marks, necessary for the main turbine exergy analysis (marked with numbers from 1 to 7). At each steam subtraction point (points 2, 4 and 6) was defined to which steam plant component (or more of them) the steam was leading during subtraction. Steam mass flow taken from the turbine during subtractions is dependable on the current steam propulsion system load, what will be further described during the measurement results presentation.

Both steam turbine cylinders were connected with the same shaft and then connected to the propulsion propeller through the gearbox which reduces propeller speed. The highest propulsion propeller speed (and thus the highest steam system load) observed in this analysis was 83.00 rpm. Propulsion propeller speed is directly proportional to steam system load.

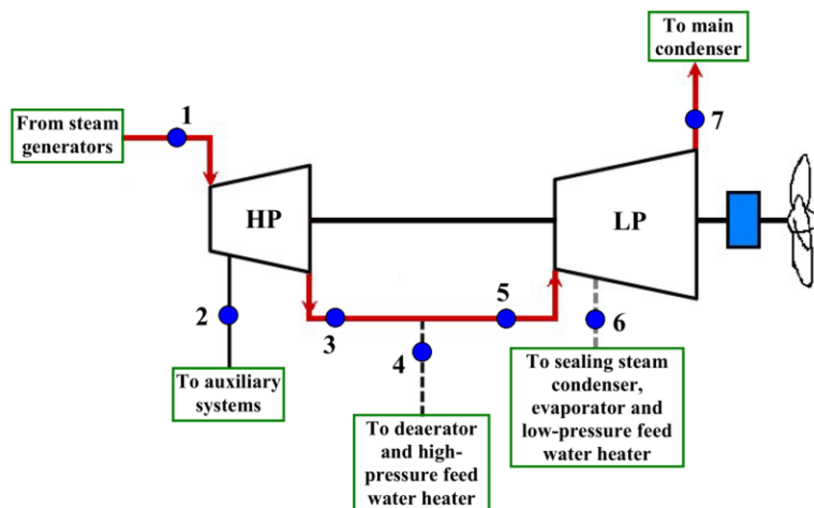


**Fig. 1** Main propulsion turbine scheme and steam flow marks

Main propulsion turbine exergy analysis will be defined by using steam stream flow marks from Fig. 1. The real (polytropic) steam expansion for the entire main propulsion turbine (both cylinders) in the  $h-s$  diagram, according to stream flow marks on the Fig. 1, is presented in Fig. 2. In the Fig. 2 was marked steam mass flows between all main turbine flow

points as well as steam mass flows subtracted from the turbine. Main turbine steam expansion end (point 7, Fig. 2) is under the saturation line, because after expansion on the main turbine, steam was led directly into the steam condenser. As turbine load increases, steam content at the LP turbine outlet (point 7) decreases.

The entire exergy analysis of the main propulsion turbine was based on the real (polytropic) steam expansion [40]. Cumulative steam mass flow lost on the turbine labyrinth seals [41] in this analysis was neglected.

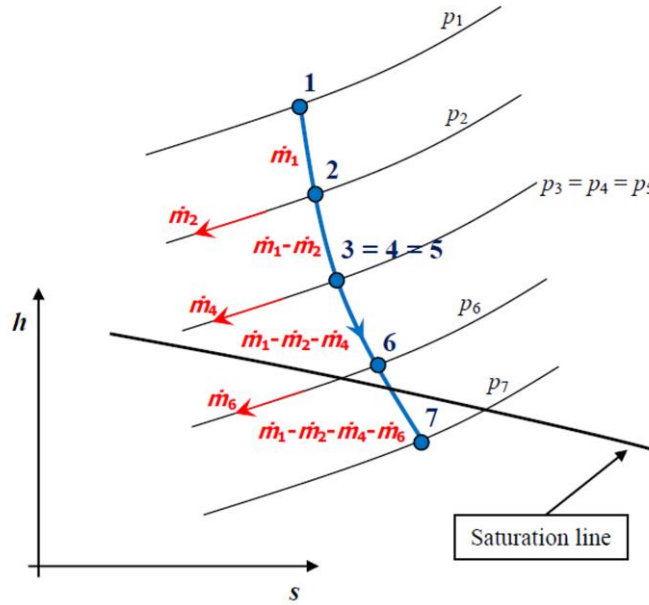


**Fig. 2** Steam expansion throughout the main propulsion turbine shown in the  $h$ - $s$  diagram (flow stream points refer to Fig. 1)

According to flow stream points and steam expansion presented in Fig. 1 and Fig. 2, mass flow balance, energy (power) and exergy balance equations for the main propulsion turbine analysis are:

- Mass flow balance:

$$\dot{m}_1 = \dot{m}_2 + \dot{m}_4 + \dot{m}_6 + \dot{m}_7 \quad (7)$$

- Exergy flow of a stream (exergy power of a stream):

$$\dot{E}_{ex,n} = \dot{m}_n \cdot \varepsilon_n = \dot{m}_n \cdot [(h_n - h_0) - T_0 \cdot (s_n - s_0)] \quad (8)$$

where index  $n$  marks steam stream flows (according to Fig. 1,  $n = 1 \dots 7$ ). The ambient state in the LNG carrier engine room during the measurements was:

pressure:  $p_0 = 0.1 \text{ MPa} = 1 \text{ bar}$ ,

temperature:  $T_0 = 25 \text{ }^\circ\text{C} = 298.15 \text{ K}$ .

- Main turbine developed power:

$$\begin{aligned} P_{\text{main turbine}} = & \dot{m}_1 \cdot (h_1 - h_2) + (\dot{m}_1 - \dot{m}_2) \cdot (h_2 - h_3) + \\ & + (\dot{m}_1 - \dot{m}_2 - \dot{m}_4) \cdot (h_5 - h_6) + (\dot{m}_1 - \dot{m}_2 - \dot{m}_4 - \dot{m}_6) \cdot (h_6 - h_7) \end{aligned} \quad (9)$$

- Main turbine lost power:

$$P_{\text{main turbine,PL}} = \dot{m}_2 \cdot (h_2 - h_3) + \dot{m}_2 \cdot (h_5 - h_6) + \dot{m}_2 \cdot (h_6 - h_7) + \dot{m}_4 \cdot (h_5 - h_6) + \dot{m}_4 \cdot (h_6 - h_7) + \dot{m}_6 \cdot (h_6 - h_7) \quad (10)$$

- Cumulative exergy power input:

$$\dot{E}_{\text{ex,IN}} = \dot{E}_{\text{ex,1}} = \dot{m}_1 \cdot \varepsilon_1 = \dot{m}_1 \cdot [(h_1 - h_0) - T_0 \cdot (s_1 - s_0)] \quad (11)$$

- Cumulative exergy power output:

$$\dot{E}_{\text{ex,OUT}} = \dot{E}_{\text{ex,2}} + \dot{E}_{\text{ex,4}} + \dot{E}_{\text{ex,6}} + \dot{E}_{\text{ex,7}} + P_{\text{main turbine}} = \dot{m}_2 \cdot \varepsilon_2 + \dot{m}_4 \cdot \varepsilon_4 + \dot{m}_6 \cdot \varepsilon_6 + \dot{m}_7 \cdot \varepsilon_7 + P_{\text{main turbine}} \quad (12)$$

- Cumulative exergy power loss (cumulative exergy destruction):

$$\begin{aligned} \dot{E}_{\text{ex,D}} &= \dot{E}_{\text{ex,IN}} - \dot{E}_{\text{ex,OUT}} = \dot{E}_{\text{ex,1}} - \dot{E}_{\text{ex,2}} - \dot{E}_{\text{ex,4}} - \dot{E}_{\text{ex,6}} - \dot{E}_{\text{ex,7}} - P_{\text{main turbine}} \\ &= \dot{m}_1 \cdot \varepsilon_1 - \dot{m}_2 \cdot \varepsilon_2 - \dot{m}_4 \cdot \varepsilon_4 - \dot{m}_6 \cdot \varepsilon_6 - \dot{m}_7 \cdot \varepsilon_7 - P_{\text{main turbine}} \end{aligned} \quad (13)$$

- Exergy efficiency:

$$\begin{aligned} \eta_{\text{ex}} &= \frac{P_{\text{main turbine}}}{\dot{E}_{\text{ex,1}} - \dot{E}_{\text{ex,2}} - \dot{E}_{\text{ex,4}} - \dot{E}_{\text{ex,6}} - \dot{E}_{\text{ex,7}}} = \\ &= \frac{P_{\text{main turbine}}}{\dot{m}_1 \cdot \varepsilon_1 - \dot{m}_2 \cdot \varepsilon_2 - \dot{m}_4 \cdot \varepsilon_4 - \dot{m}_6 \cdot \varepsilon_6 - \dot{m}_7 \cdot \varepsilon_7} \end{aligned} \quad (14)$$

Steam specific enthalpies and specific entropies were calculated from measured steam pressures and temperatures of each flow stream by using NIST REFPROP software [42].

### 2.3 Entire marine steam power plant exergy efficiency and destruction

Total exergy destruction of the entire steam power plant (any steam power plant), according to [27] and [31], is the sum of exergy destructions of all components and can be calculated by using an equation:

$$\dot{E}_{\text{ex,D,plant}} = \sum \dot{E}_{\text{ex,D}}(\text{all components}) \quad (15)$$

while the entire steam power plant exergy efficiency can be calculated as:

$$\eta_{\text{ex,plant}} = \frac{P_{\text{produced power}}}{\dot{E}_{\text{ex,fuel}}} = \frac{P_{\text{main turbine}}}{\dot{m}_{\text{fuel}} \cdot \varepsilon_{\text{fuel}}} \quad (16)$$

In land-based steam power plants produced power is main steam turbine power. If the land-based steam power plant has auxiliary steam turbines, their power is usually much lower than the power produced by main turbine, so the power of auxiliary steam turbines in such steam power plants can be neglected in the equation (16).

For the marine steam power plant at LNG carrier in which analyzed main propulsion turbine operates, exergy destruction of the entire plant can be calculated as presented in equation (15). The equation for exergy efficiency calculation of the entire marine steam power plant at LNG carrier should be modified when compared to equation (16) because of two reasons.

The first reason is that in the marine steam power plant at analyzed LNG carrier along with main propulsion steam turbine operates three auxiliary steam turbines (two turbo-

generators and steam turbine for the main feed water pump drive). Cumulative power produced by auxiliary steam turbines in some marine steam plant operating regimes can notably influenced total produced power. The second reason of the equation (16) correction for the analyzed marine steam power plant at LNG carrier is that both marine steam generators simultaneously use two fuels - heavy fuel oil (HFO) and LNG. Therefore, the equation of exergy efficiency calculation for the entire marine steam power plant at the analyzed LNG carrier, in any load, will be:

$$\eta_{ex,plant} = \frac{P_{main\ turbine} + P_{turbo-generator1} + P_{turbo-generator2} + P_{pump}}{\dot{m}_{HFO} \cdot \varepsilon_{HFO} + \dot{m}_{LNG} \cdot \varepsilon_{LNG}} \quad (17)$$

For equation (17) it should be noted that power produced by the main steam turbine is the most dominant one during the majority of marine steam power plant operation. HFO and LNG mass flows in equation (17) are cumulative mass flows for both steam generators, while specific exergies of both fuels can be calculated from fuel mass fractions.

Analyzed main propulsion steam turbine from LNG carrier doesn't have steam re-heating. Therefore, for such entire marine steam propulsion plant can be expected exergy efficiencies between 12 % and 15 % at low main turbine load, around 20 % at middle main turbine load and between 25 % and 30 % at high main turbine load. For comparison, similar marine steam propulsion plant from LNG carrier where main turbine posses steam re-heating has plant exergy efficiency of around 34 % at high main turbine load [16].

### 3. Main propulsion turbine measurement results and measuring equipment

Measurement results of required steam operating parameters (pressure, temperature and mass flow) for main propulsion steam turbine, according to steam flows – Fig. 1, are presented in relation to the propulsion propeller speed, Table 2 and Table 3. Propulsion propeller speed is directly proportional to main propulsion turbine load, higher propulsion propeller speed denotes a higher steam turbine load. In Table 2 are presented measurements for HP turbine cylinder, while in Table 3 are presented measurements for LP turbine cylinder.

**Table 2** Main propulsion turbine measurement results – HP cylinder

Stream flow mark (Fig. 1)	Propulsion propeller speed (rpm)	Steam mass flow at the HP turbine entrance (kg/h)	Steam temperature at the HP turbine entrance (°C)	Steam pressure at the HP turbine entrance (MPa)
1	41.78	16605	488.0	6.190
	74.59	65012	513.5	6.020
	83.00	96474	500.0	5.899
Stream flow mark (Fig. 1)	Propulsion propeller speed (rpm)	Steam mass flow of HP turbine subtraction (kg/h)	Steam temperature of HP turbine subtraction (°C)	Steam pressure of HP turbine subtraction (MPa)
2	41.78	0	-	-
	74.59	0	-	-
	83.00	3268	350.0	1.565
Stream flow mark (Fig. 1)	Propulsion propeller speed (rpm)	Steam mass flow at the HP turbine outlet (kg/h)	Steam temperature at the HP turbine outlet (°C)	Steam pressure at the HP turbine outlet (MPa)
3	41.78	16605	243.0	0.151
	74.59	65012	256.0	0.467
	83.00	93206	256.0	0.593

**Table 3** Main propulsion turbine measurement results – LP cylinder

Stream flow mark (Fig. 1)	Propulsion propeller speed (rpm)	Subtraction steam mass flow between HP and LP turbine (kg/h)	Subtraction steam temperature between HP and LP turbine (°C)	Subtraction steam pressure between HP and LP turbine (MPa)
4	41.78	0	-	-
	74.59	4690	256.0	0.467
	83.00	13609	256.0	0.593
Stream flow mark (Fig. 1)	Propulsion propeller speed (rpm)	Steam mass flow at the LP turbine entrance (kg/h)	Steam temperature at the LP turbine entrance (°C)	Steam pressure at the LP turbine entrance (MPa)
5	41.78	16605	243.0	0.151
	74.59	60322	256.0	0.467
	83.00	79597	256.0	0.593
Stream flow mark (Fig. 1)	Propulsion propeller speed (rpm)	Steam mass flow of LP turbine subtraction (kg/h)	Steam temperature of LP turbine subtraction (°C)	Steam pressure of LP turbine subtraction (MPa)
6	41.78	0	-	-
	74.59	2032	156.0	0.097
	83.00	3355	153.0	0.121
Stream flow mark (Fig. 1)	Propulsion propeller speed (rpm)	Steam mass flow at the LP turbine outlet (kg/h)	Steam temperature at the LP turbine outlet (°C)	Steam pressure at the LP turbine outlet (MPa)
7	41.78	16605	32.50	0.00489
	74.59	58290	29.47	0.00412
	83.00	76242	34.92	0.00561

Measurement results were obtained from the existing measuring equipment mounted on both main propulsion turbine cylinders and on all steam subtraction streams. List of used measuring equipment was presented in Table 4.

**Table 4** Main propulsion turbine measuring equipment

Stream flow mark (Fig. 1)	Steam mass flow (differential pressure transmitters [43])	Steam pressure (pressure transmitters [44])	Steam temperature (immersion probes [45])
1	Yamatake JTD960A	Yamatake JTG960A	Greisinger GTF 601-Pt100
2	Yamatake JTD960A	Yamatake JTG940A	Greisinger GTF 601-Pt100
3	Yamatake JTD930A	Yamatake JTG940A	Greisinger GTF 401-Pt100
4	Yamatake JTD930A	Yamatake JTG940A	Greisinger GTF 401-Pt100
5	Yamatake JTD930A	Yamatake JTG940A	Greisinger GTF 401-Pt100
6	Yamatake JTD920A	Yamatake JTG940A	Greisinger GTF 401-Pt100
7	Yamatake JTD910A	Yamatake JTG940A	Greisinger GTF 401-Pt100
Propulsion propeller speed	Kyma Shaft Power Meter (KPM-PFS) [46]		

#### 4. Main propulsion turbine exergy analysis results with the discussion

Cumulative exergy power input and output of the main propulsion turbine at different propulsion propeller speeds, calculated by using equations (11) and (12) are presented in Fig. 3. Main turbine cumulative exergy power input and output increases during the increase in propulsion propeller speed (increase in steam system load). The difference between main turbine cumulative exergy power input and output also increases during the increase in propulsion propeller speed, what defines main turbine exergy power losses (exergy destruction).

At the lowest observed propulsion propeller speed of 41.78 rpm, main turbine cumulative exergy power input amounts 6277 kW, while cumulative exergy power output amounts 4236 kW. At propulsion propeller speed of 74.59 rpm cumulative main turbine exergy power input and output amounts 25205 kW and 20098 kW, while at 83.00 rpm cumulative exergy power input and output amounts 36824 kW and 30901 kW. Presented exergy power inputs and outputs in Fig. 3 for every propulsion propeller speed are valid for the ambient state in the LNG carrier engine room during measurements.

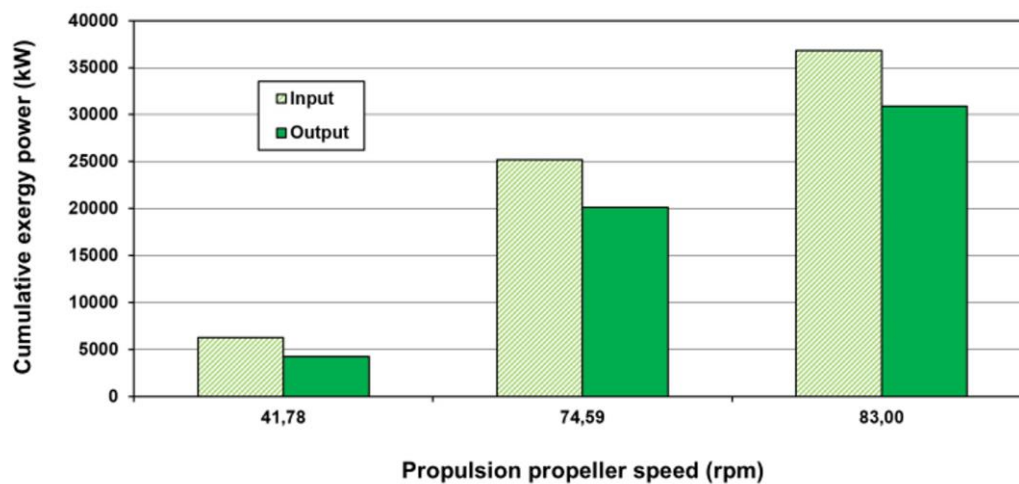


**Fig. 3** Main propulsion turbine cumulative exergy power input and output at different propulsion propeller speeds - according to measurement state

Main propulsion turbine cumulative exergy destruction and exergy efficiency are directly proportional - both increases during the increase in propulsion propeller speed, Fig. 4. According to equation (13), increase in main turbine cumulative exergy destruction during the increase in turbine load is caused by a fact that cumulative exergy power input increases faster than cumulative exergy power output. Main turbine exergy efficiency also increases during the increase in turbine load because turbine developed power increases faster than the difference in exergy flows between turbine inlet and outlet, equation (14).

In the observed main turbine load range, cumulative exergy destruction and exergy efficiency amounts 2041 kW and 66.01 % at propulsion propeller speed of 41.78 rpm after which increases to 5107 kW and 78.12 % at 74.59 rpm. At the highest observed turbine load (at the highest observed propulsion propeller speed) cumulative turbine exergy destruction and efficiency are the highest and amounts 5923 kW and 80.72 %.

When the analyzed marine propulsion steam turbine is compared with high power steam turbines from land-based thermal power plants such as turbines in [47] and [48], it can be concluded that analyzed marine turbine has higher exergy destruction in regards to developed power, while its exergy efficiency is lower. Compared to high power steam turbines, marine propulsion steam turbine must be much flexible in operation, especially during maneuvering

in ports, so its lower exergy efficiency and higher exergy destruction in regards to developed power are expected.

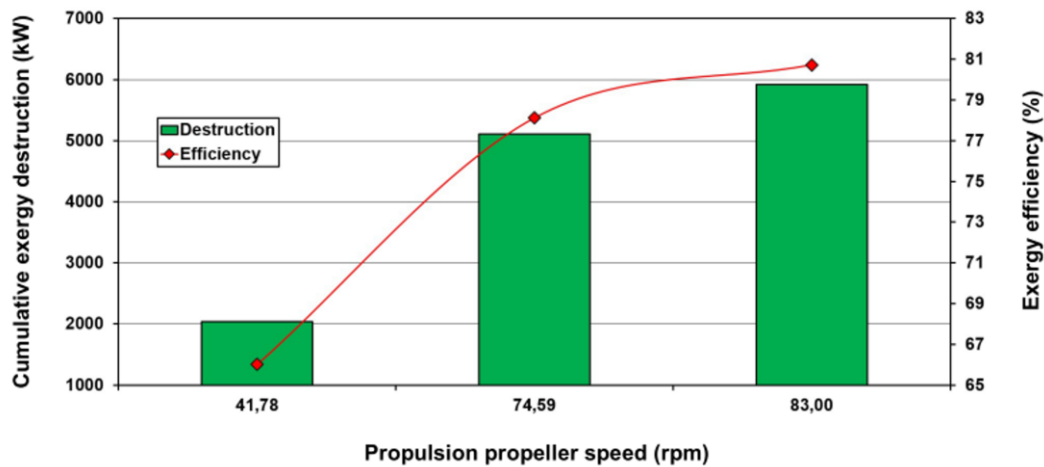


**Fig. 4** Change in main turbine cumulative exergy destruction and exergy efficiency at different propulsion propeller speeds - according to measurement state

Main propulsion turbine developed power is calculated by using measured steam mass flows and steam specific enthalpies obtained from measured steam pressures and temperatures, equation (9). Increase in propulsion propeller speed resulted in an increase in analyzed turbine developed power, Fig. 5. At the lowest observed propulsion propeller speed of 41.78 rpm, main turbine developed power amounts 3964 kW after which increases to 18232 kW at 74.59 rpm and at the highest observed propulsion propeller speed of 83.00 rpm turbine developed power amounts 24805 kW. Turbine developed power is an essential element for proper defining cumulative turbine exergy power output, exergy destruction and exergy efficiency, equations (12), (13) and (14). An increase in turbine developed power during the increase in propulsion propeller speed is expected, because measurements of required operating parameters for exergy analysis were performed while LNG carrier leaving the port (41.78 rpm) until the ship reaches its usual navigation speed at open sea (83.00 rpm).

Turbine lost power, defined by an equation (10), is an additional main turbine power which can be developed if the steam was not subtracted from the turbine. If the steam subtractions were closed, additional steam mass flow will expand through the both turbine cylinders (HP and LP) between the same steam specific enthalpies (obtained from measured steam pressure and temperature) and thus more power will be produced. Main turbine steam subtractions are calculated in detail, to ensure continuous steam supply from the main turbine to all necessary steam consumers in the propulsion plant. If the steam subtractions were not in operation, especially at high turbine loads, it is questionable whether the power plant could operate at all.

Therefore, turbine lost power represents the additional power which can be developed for propulsion propeller drive if necessary. Analyzed main propulsion turbine operates in a manner that on lower loads (41.78 rpm) steam subtractions were closed (Table 2 and Table 3) and turbine lost power is equal to 0 kW, Fig. 5. At lower steam plant loads, steam consumers get the necessary amount of steam directly from steam generators.

Increase in steam system and consequentially main turbine load resulted with steam subtractions opening. Steam mass flow subtracted from the main propulsion turbine increases proportionally with an increase in turbine load. As a result, turbine lost power at propulsion propeller speed of 74.59 rpm amounts 987 kW, while at the highest propulsion propeller speed of 83.00 rpm turbine lost power is the highest and amounts 3339 kW because at the

83.00 rpm all steam subtractions are opened and the steam mass flow subtracted from the main turbine is the highest.

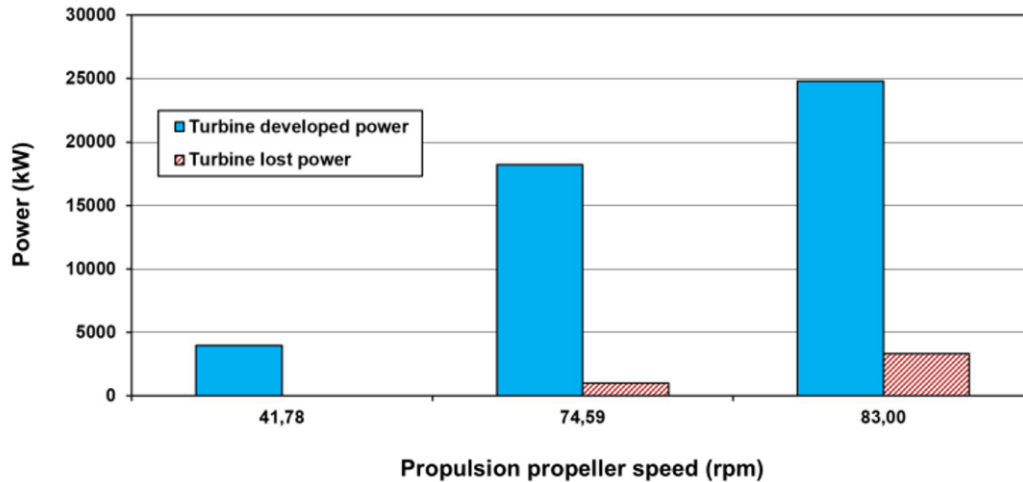


Fig. 5 Main turbine developed and lost power at different propulsion propeller speeds

After expansion in main propulsion turbine cylinders, at the turbine outlet, steam was led directly to the main steam condenser (point 7, Fig. 1). To be able to liquefy that steam in the condenser, its operating parameters must be under the saturation line, in the area of saturated steam. It is interesting to observe the change of steam content at the main turbine outlet, according to measured data from Table 3.

At the lowest propulsion propeller speed of 41.78 rpm, steam content at the main turbine outlet is high and amounts 98.83 %, Fig. 6. Increase in main turbine load resulted with a decrease in steam content at the turbine outlet. At the main turbine outlet, steam content of 93.23 % was observed at propulsion propeller speed of 74.59 rpm, while at the highest load (83.00 rpm) steam content is the lowest and amounts 92.10 %.

The majority of LNG carrier operation during the whole exploitation period can be expected at the highest steam system load (and thus at the highest main turbine load). As presented in Fig. 6, at the highest loads the amount of water droplets in the steam after turbine will be the highest. High amount of water droplets will lead to increased erosion on the turbine rotor blades, especially on the last stages of the LP turbine cylinder. Therefore, the rotor blades at the last few stages of LP turbine are covered with special protective linings made of hard materials (usually stellite) for wear protection in order to prolong their replacement period [49,50].

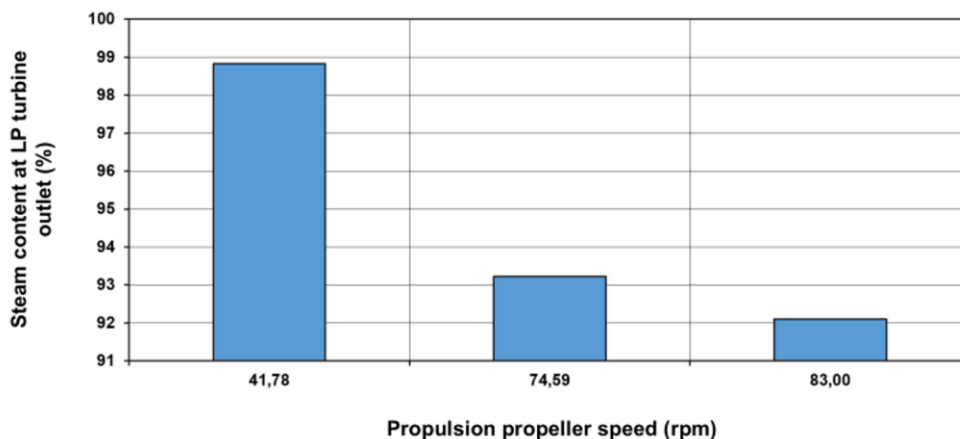


Fig. 6 Change in steam content at LP turbine outlet during the increase in propulsion propeller speed

Exergy flow streams at each main propulsion turbine stream point, according to Fig. 1, for each observed propulsion propeller speed are presented in Fig. 7. Exergy flow stream at each turbine stream point is calculated by using equation (8) and measured operating data (engine room ambient state). The best explanation of Fig. 7 is to analyze exergy flow streams at each propulsion propeller speed.

At the lowest propulsion propeller speed of 41.78 rpm, exergy flow stream at the turbine inlet (point 1, Fig. 1) amounts 6277 kW. At this propulsion propeller speed all turbine subtractions are closed and exergy flow streams are equal to zero (point 2, 4 and 6, Fig. 1). At the HP turbine cylinder outlet (point 3) exergy flow stream amounts 2922 kW and the same exergy flow stream enters in the LP turbine cylinder, Fig. 7. At the LP cylinder outlet (at the main turbine outlet), exergy flow stream at 41.78 rpm amounts only 272 kW.

The exergy flow stream at the turbine inlet (point 1) at 74.59 rpm is significantly higher in comparison with the lower propulsion propeller speed and amounts 25205 kW, Fig. 7. Steam subtraction at the HP turbine cylinder (point 2) is closed also at 74.59 rpm. At the HP turbine cylinder outlet (point 3), exergy flow stream amounts 14338 kW. At the LP turbine cylinder inlet (point 5), exergy flow stream amounts 13304 kW what is lower than an exergy flow stream at the HP turbine cylinder outlet (point 3) for exergy flow stream subtracted between HP and LP turbine cylinders which amounts 1034 kW (point 4) at this propulsion propeller speed. At the LP turbine cylinder subtraction (point 6) exergy flow stream amounts 288 kW and finally, at the LP turbine cylinder outlet (point 7) exergy flow stream is equal to 543 kW. If compared propulsion propeller speeds of 41.78 rpm and 74.59 rpm, exergy flow streams are significantly higher at higher propulsion propeller speed for each turbine stream point (with an exception of HP turbine cylinder subtraction which is closed in both cases).

The highest exergy flow streams at each turbine stream point can be observed at the highest propulsion propeller speed of 83.00 rpm, Fig. 7, although the difference in propulsion propeller speeds of 74.59 rpm and 83.00 rpm is not significant. At the turbine inlet (point 1) exergy flow stream amounts 36824 kW at 83.00 rpm. Only at the highest observed propulsion propeller speed, steam subtraction at the HP turbine cylinder (point 2) is open and exergy flow stream at this subtraction amounts 944 kW. At the LP turbine cylinder inlet (point 5), exergy flow stream amounts 18228 kW, what is lower than an exergy flow stream at the HP cylinder outlet (point 3) which amounts 21344 kW for exergy flow stream subtracted between HP and LP turbine cylinders (point 4). The last subtraction at the LP turbine cylinder (point 6) takes an exergy flow stream equal to 502 kW, while at the turbine outlet (at the LP cylinder outlet, point 7) exergy flow stream amounts 1534 kW for a propulsion propeller speed of 83.00 rpm.

Presented change leads to a conclusion that exergy flow streams can vary considerably, even for a small difference in propulsion propeller speed. Likewise, exergy flow streams are directly proportional to analyzed turbine load, they increase at each stream point during the increase in turbine load.

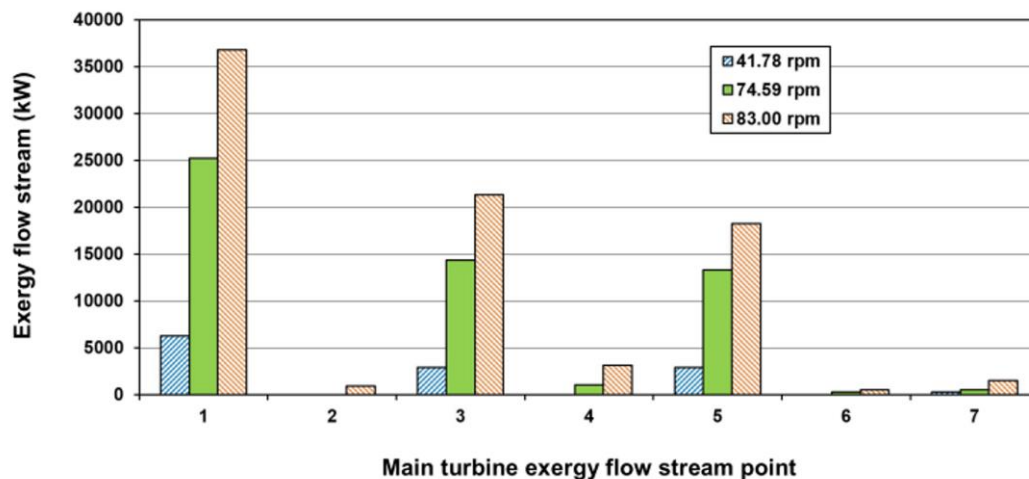


**Fig. 7** Main turbine exergy flow streams at each turbine stream point for each observed propulsion propeller speed (exergy flow stream points refer to Fig. 1)

Exergy destruction and exergy efficiency (as well as exergy flow streams) of any steam plant component depend on the ambient pressure and temperature. Real change in the ambient pressure is small and the influence of the ambient pressure change on exergy efficiency or exergy destruction of any steam plant component can be neglected [51]. The ambient temperature change, in practically expected ranges, can have a significant influence on some steam plant components exergy destruction and exergy efficiency.

Some researchers as Ahmadi and Toghraie [28], Ameri et al. [38], Aljundi [52] and Kopac and Hilalci [53] investigate the influence of the ambient temperature on several steam plant components from land-based steam power plants. In each analysis one of the observed components was high power steam turbine and it was investigated the ambient temperature influence on high power steam turbine exergy efficiency and exergy power losses (exergy destruction). All researchers concluded that the ambient temperature change has low impact on high power steam turbines exergy destruction and exergy efficiency. The ambient temperature increase causes an increase in steam turbine exergy destruction and a decrease in steam turbine exergy efficiency. Usually, an increase in the ambient temperature of 10 °C causes a decrease in high power steam turbine exergy efficiency for about 1 % or less.

It can be expected that the influence of the ambient temperature on exergy destruction and exergy efficiency of marine main propulsion steam turbine will also have low impact. Ambient temperature of marine propulsion steam plants usually has a greater influence on exergy destruction and exergy efficiency of plant components when compared to the land-based plants, depending greatly on the geographic area in which ship operates. Likewise, marine steam propulsion plants are more frequently affected by different ambient temperatures than land-based steam plants.

In this analysis, the ambient temperature was varied from 10 °C to 40 °C in the steps of 10 °C, while the ambient pressure remains constant as at the measurement state (1 bar). Selected ambient temperature range can be expected in the wider operating range of the analyzed LNG carrier.

Main propulsion turbine cumulative exergy destruction change during the ambient temperature variation in all three observed propulsion propeller speeds is presented in Fig. 8. As for high power steam turbines from land-based steam power plants, for the analyzed

marine propulsion turbine cumulative exergy destruction increases during the increase in the ambient temperature, at each observed turbine load.

At propulsion propeller speed of 41.78 rpm, turbine cumulative exergy destruction is the lowest and amounts 1938 kW at the ambient temperature of 10 °C, while at the highest observed ambient temperature of 40 °C turbine cumulative exergy destruction is the highest and amounts 2143 kW. An increase in the ambient temperature for 10 °C causes an average increase in turbine cumulative exergy destruction of 68 kW at this propulsion propeller speed.

At 74.59 rpm, turbine cumulative exergy destruction increases from 4851 kW at the ambient temperature of 10 °C to 5363 kW at the ambient temperature of 40 °C. An increase in the ambient temperature for 10 °C causes an average increase in turbine cumulative exergy destruction of 171 kW at this propulsion propeller speed.

Finally, at the highest main propulsion turbine load (83.00 rpm), exergy destruction increases from 5627 kW at the ambient temperature of 10 °C to 6220 kW at the ambient temperature of 40 °C. An increase in the ambient temperature for 10 °C causes an average increase in turbine cumulative exergy destruction of 198 kW at this propulsion propeller speed.

For the analyzed marine propulsion steam turbine is also valid a conclusion that the average increase in cumulative exergy destruction during the ambient temperature increase is bigger and bigger as turbine load increases. Ambient temperature change does not have a significant impact on the analyzed turbine cumulative exergy destruction.

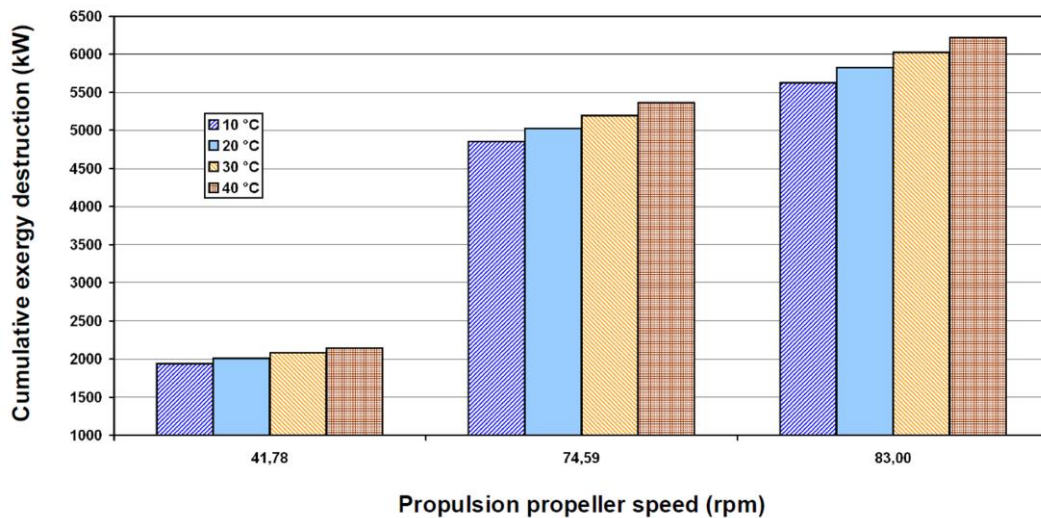


**Fig. 8** Change in main turbine cumulative exergy destruction during the ambient temperature variation at different propulsion propeller speeds

Analyzed main propulsion turbine exergy efficiency change during the change in the ambient temperature is presented in Fig. 9 for each observed propulsion propeller speed. Marine turbine exergy efficiency decreases during the increase in the ambient temperature for each propulsion propeller speed, so the change is the same as for high power steam turbines from land-based steam power plants.

The highest main propulsion turbine exergy efficiency can be observed at the lowest ambient temperature of 10 °C at each turbine load. At the lowest observed ambient temperature of 10 °C analyzed turbine exergy efficiency amounts 67.16 % at 41.78 rpm, 78.99 % at 74.59 rpm and 81.51 % at the highest propulsion propeller speed of 83.00 rpm. At the highest observed ambient temperature of 40 °C marine propulsion turbine exergy efficiency is the lowest for each turbine load and amounts 64.91 % at 41.78 rpm, 77.27 % at

74.59 rpm and 79.95 % at 83.00 rpm. An increase in the ambient temperature for 10 °C causes average decrease in marine propulsion turbine exergy efficiency of 0.75 % at 41.78 rpm, 0.57 % at 74.59 rpm and 0.52 % at 83.00 rpm.

For the analyzed marine steam turbine is valid a conclusion that the average decrease in exergy efficiency during the ambient temperature increase is as lower as turbine load increases. The ambient temperature change does not have significant impact also on the marine propulsion turbine exergy efficiency.

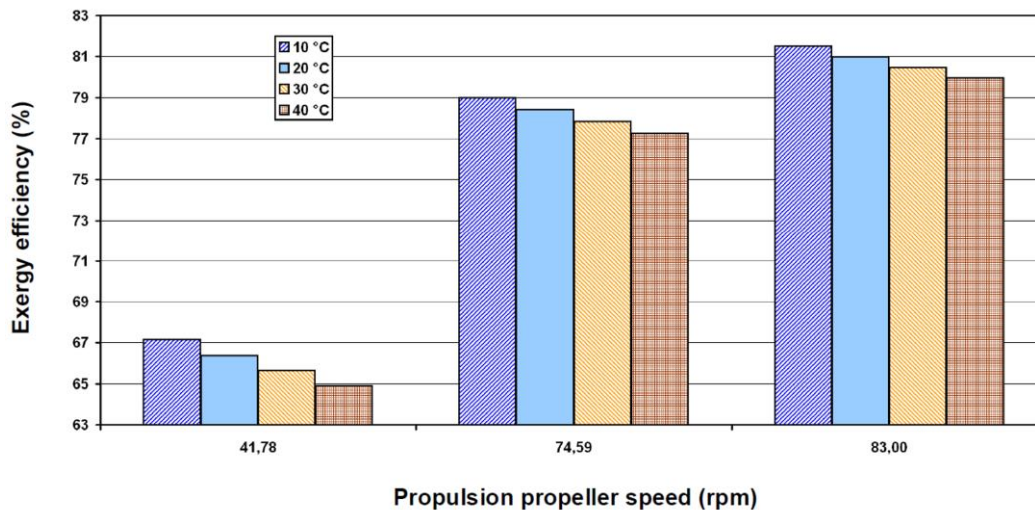


**Fig. 9** Change in main turbine exergy efficiency during the ambient temperature variation at different propulsion propeller speeds

## 5. Conclusion

This paper presents an exergy analysis of main propulsion steam turbine from LNG carrier steam propulsion plant at three different turbine loads (low load - 41.78 rpm, middle load - 74.59 rpm and high load - 83.00 rpm). Analyzed turbine cumulative exergy destruction and exergy efficiency are directly proportional. The lowest turbine cumulative exergy destruction and exergy efficiency amounts 2041 kW and 66.01 % at propulsion propeller speed of 41.78 rpm, while the highest cumulative exergy destruction and exergy efficiency amounts 5923 kW and 80.72 % at 83.00 rpm. The analyzed marine steam turbine has higher cumulative exergy destruction in regards to developed power and lower exergy efficiency when compared with high power steam turbines from land-based thermal power plants.

Turbine lost power is defined with steam mass flows subtracted from the turbine and represents the additional power which can be developed for propulsion propeller drive if necessary. Analyzed turbine lost power at the highest propulsion propeller speed of 83.00 rpm is the highest and amounts 3339 kW. Steam content at the main propulsion turbine outlet (main condenser inlet) decreases during the increase in propulsion propeller speed. Analyzed turbine exergy flow streams can vary considerably, even for a small difference in propulsion propeller speed. The ambient temperature change does not affect significantly exergy efficiency or destruction of main marine propulsion steam turbine - what is an identical conclusion as for high power steam turbines from land-based steam power plants.

This analysis presented that LNG carrier crew should avoid running at partial main turbine loads during a major period of time - main turbine exergy efficiency significantly decreases at partial loads. Steam subtractions opening and turbine lost power at high loads leads to a possibility of turbine optimization. During the significant ambient temperature increase (for example summer operation in the Persian Gulf), the main propulsion steam

turbine is not the component for which can be expected notable decrease in efficiency or increase in losses.

### Acknowledgment

The authors would like to extend their appreciations to the main ship-owner office for conceding measuring equipment and for all help during the exploitation measurements. A retired professor Vladimir Medica, Faculty of Engineering, University of Rijeka is gratefully acknowledged for helpful suggestions and discussions. This work has been fully supported by the Croatian Science Foundation under the project IP-2018-01-3739.

<b><u>NOMENCLATURE</u></b>		<b>Greek symbols:</b>	
<b>Abbreviations:</b>		$\varepsilon$	specific exergy, kJ/kg
HFO	Heavy Fuel Oil	$\eta$	efficiency, -
HP	High Pressure	<b>Subscripts:</b>	
LNG	Liquefied Natural Gas	0	ambient state
LP	Low Pressure	D	destruction
<b>Latin Symbols:</b>		ex	exergy
$\dot{E}$	stream flow power, kJ/s	IN	inlet (input)
$h$	specific enthalpy, kJ/kg	OUT	outlet (output)
$\dot{m}$	mass flow rate, kg/s or kg/h	PL	power lost
$p$	pressure, MPa		
$P$	power, kJ/s		
$\dot{Q}$	heat transfer, kJ/s		
$s$	specific entropy, kJ/kg·K		
$\dot{X}_{\text{heat}}$	heat exergy transfer, kJ/s		
$T$	temperature, °C or K		

### REFERENCES

- [1] Senčić, T., Račić, N., Franković, B.: *Influence of Low-Speed Marine Diesel Engine Settings on Waste Heat Availability*, Shipbuilding: Theory and Practice of Naval Architecture, Marine Engineering and Ocean Engineering Vol. 63., No. 4, p. 329-335, 2012. (UDC 621.436:629.5)
- [2] Zhao, F., Yang, W., Tan, W. W., Yu, W., Yang, J., Chou, S. K.: *Power management of vessel propulsion system for thrust efficiency and emissions mitigation*, Applied Energy 161, p. 124–132, 2016. <https://doi.org/10.1016/j.apenergy.2015.10.022>
- [3] Mrzljak, V., Medica, V., Bukovac, O.: *Volume agglomeration process in quasi-dimensional direct injection diesel engine numerical model*, Energy 115, p. 658-667, 2016. <https://doi.org/10.1016/j.energy.2016.09.055>
- [4] Bukovac, O., Medica, V., Mrzljak, V.: *Steady state performances analysis of modern marine two-stroke low speed diesel engine using MLP neural network model*, Shipbuilding: Theory and Practice of Naval Architecture, Marine Engineering and Ocean Engineering Vol. 66., No. 4, p. 57-70, 2015. (UDC 629.54:621.436.13:519.6)

- [5] Attah, E. E., Bucknall, R.: *An analysis of the energy efficiency of LNG ships powering options using the EEDI*, Ocean Engineering 110, Part B, p. 62–74, 2015. (doi:10.1016/j.oceaneng.2015.09.040)
- [6] Fernández, I. A., Gómez, M. R., Gómez, J. R., Insua, A. A. B.: *Review of propulsion systems on LNG carriers*, Renewable and Sustainable Energy Reviews 67, p. 1395–1411, 2017. <https://doi.org/10.1016/j.rser.2016.09.095>
- [7] Mrzljak, V., Poljak, I., Medica-Viola, V.: *Dual fuel consumption and efficiency of marine steam generators for the propulsion of LNG carrier*, Applied Thermal Engineering, 119, p. 331–346, 2017. <https://doi.org/10.1016/j.applthermaleng.2017.03.078>
- [8] Mrzljak, V., Poljak, I., Mrakovčić, T.: *Energy and exergy analysis of the turbo-generators and steam turbine for the main feed water pump drive on LNG carrier*, Energy Conversion and Management, 140, p. 307–323, 2017. <https://doi.org/10.1016/j.enconman.2017.03.007>
- [9] Taylor, D. A.: *Introduction to Marine Engineering*, Elsevier Butterworth-Heinemann, 1998.
- [10] Medica-Viola, V., Pavković, B., Mrzljak, V.: *Numerical model for on-condition monitoring of condenser in coal-fired power plants*, International Journal of Heat and Mass Transfer 117, p. 912–923, 2018. <https://doi.org/10.1016/j.ijheatmasstransfer.2017.10.047>
- [11] Baawain, M., Choudri, B. S., Ahmed, M., Purnama, A.: *Recent Progress in Desalination, Environmental and Marine Outfall Systems*, Springer International Publishing Switzerland, 2015. <https://doi.org/10.1007/978-3-319-19123-2>
- [12] Mrzljak, V., Poljak, I., Medica-Viola, V.: *Energy and Exergy Efficiency Analysis of Sealing Steam Condenser in Propulsion System of LNG Carrier*, Our Sea, International Journal of Maritime Science & Technology, Vol. 64., No. 1, p. 20-25, 2017. <https://doi.org/10.17818/NM/2017/1.4>
- [13] Mrzljak, V., Poljak, I., Medica-Viola, V.: *Efficiency and losses analysis of low-pressure feed water heater in steam propulsion system during ship maneuvering period*, Scientific Journal of Maritime Research Vol. 30., No. 2, p. 133-140, 2016. <https://doi.org/10.31217/p.30.2.6>
- [14] Mrzljak, V., Poljak, I., Medica-Viola, V.: *Thermodynamical analysis of high-pressure feed water heater in steam propulsion system during exploitation*, Shipbuilding: Theory and Practice of Naval Architecture, Marine Engineering and Ocean Engineering Vol. 68., No. 2, p. 45-61, 2017. <https://doi.org/10.21278/brod68204>
- [15] Moran M., Shapiro H., Boettner, D. D., Bailey, M. B.: *Fundamentals of engineering thermodynamics*, Seventh edition, John Wiley and Sons, Inc., 2011.
- [16] Koroglu, T., Sogut, O. S.: *Conventional and Advanced Exergy Analyses of a Marine Steam Power Plant*, Energy 163, p. 392-403, 2018. <https://doi.org/10.1016/j.energy.2018.08.119>
- [17] Cengel Y., Boles M.: *Thermodynamics an engineering approach*, Eighth edition, McGraw-Hill Education, 2015.
- [18] Sutton, I.: *Plant Design and Operations*, Elsevier Inc., 2015.
- [19] Chang, D., Rhee, T., Nam, K., Chang, K., Lee, D., Jeong, S.: *A study on availability and safety of new propulsion systems for LNG carriers*, Reliability Engineering and System Safety 93, p. 1877– 1885, 2008. <https://doi.org/10.1016/j.ress.2008.03.013>
- [20] Schinas, O., Butler, M.: *Feasibility and commercial considerations of LNG-fueled ships*, Ocean Engineering 122, p. 84–96, 2016. <https://doi.org/10.1016/j.oceaneng.2016.04.031>
- [21] Senary, K., Tawfik, A., Hegazy, E., Ali, A.: *Development of a waste heat recovery system onboard LNG carrier to meet IMO regulations*, Alexandria Engineering Journal 55, Issue 3, p. 1951–1960, 2016. <https://doi.org/10.1016/j.aej.2016.07.027>
- [22] Ammar, N. R., Seddiek, I. S.: *Eco-environmental analysis of ship emission control methods: Case study RO-RO cargo vessel*, Ocean Engineering 137, p. 166–173, 2017. <https://doi.org/10.1016/j.oceaneng.2017.03.052>
- [23] Raj, R., Ghandehariun, S., Kumar, A., Geng, J., Ma, L.: *A techno-economic study of shipping LNG to the Asia-Pacific from Western Canada by LNG carrier*, Journal of Natural Gas Science and Engineering 34, p. 979–992, 2016. <https://doi.org/10.1016/j.jngse.2016.07.024>
- [24] Vanem, E., Antao, P., Østvik, I., Del Castillo de Comas, F.: *Analysing the risk of LNG carrier operations*, Reliability Engineering and System Safety 93, p. 1328–1344, 2008. <https://doi.org/10.1016/j.ress.2007.07.007>
- [25] Baldi, F., Johnson, H., Gabriellii, C., Andersson, K.: *Energy and Exergy Analysis of Ship Energy Systems – The Case study of a Chemical Tanker*, International Journal of Thermodynamics 18 (2), p. 82-93, 2015. (doi:10.5541/ijot.70299)

- [26] Baldi, F., Ahlgren, F., Van Nguyen, T., Thern, M., Andersson, K.: *Energy and Exergy Analysis of a Cruise Ship*, *Energies* 2018, 11, 2508 <https://doi.org/10.3390/en11102508>
- [27] Erdem, H.H., Akkaya, A.V., Cetin, B., Dagdas, A., Sevilgen, S.H., Sahin, B., Teke, I., Gungor, C., Atas, S.: *Comparative energetic and exergetic performance analyses for coal-fired thermal power plants in Turkey*, *International Journal of Thermal Sciences*, 48, p. 2179–2186, 2009. <https://doi.org/10.1016/j.ijthermalsci.2009.03.007>
- [28] Ahmadi, G. R., Toghraie, D.: *Energy and exergy analysis of Montazeri Steam Power Plant in Iran*, *Renewable and Sustainable Energy Reviews*, 56, p. 454–463, 2016. <https://doi.org/10.1016/j.rser.2015.11.074>
- [29] Kanoğlu, M., Çengel, Y.A., Dincer, I.: *Efficiency Evaluation of Energy Systems*, Springer Briefs in Energy, Springer, 2012. <https://doi.org/10.1007/978-1-4614-2242-6>
- [30] Mrzljak, V., Poljak, I., Žarković, B.: *Exergy Analysis of Steam Pressure Reduction Valve in Marine Propulsion Plant on Conventional LNG Carrier*, *International Journal of Maritime Science & Technology "Our Sea"* 65(1), p. 24–31, 2018. <https://doi.org/10.17818/NM/2018/1.4>
- [31] Ahmadi, G., Toghraie, D., Azimian, A., Ali Akbari, O.: *Evaluation of synchronous execution of full repowering and solar assisting in a 200 MW steam power plant, a case study*, *Applied Thermal Engineering*, 112, p. 111–123, 2017. <https://doi.org/10.1016/j.applthermaleng.2016.10.083>
- [32] Hafdhi, F., Khir, T., Ben Yahyia, A., Ben Brahim, A.: *Energetic and exergetic analysis of a steam turbine power plant in an existing phosphoric acid factory*, *Energy Conversion and Management*, 106, p. 1230–1241, 2015. <https://doi.org/10.1016/j.enconman.2015.10.044>
- [33] Jokandan, M.J., Aghbashlo, M., Mohtasebi, S.S.: *Comprehensive exergy analysis of an industrial-scale yogurt production plant*, *Energy* 93, p. 1832–1851, 2015. <https://doi.org/10.1016/j.energy.2015.10.003>
- [34] Tan, H., Shan, S., Nie, Y., Zhao, Q.: *A new boil-off gas re-liquefaction system for LNG carriers based on dual mixed refrigerant cycle*, *Cryogenics* 92, p. 84–92, 2018. <https://doi.org/10.1016/j.cryogenics.2018.04.009>
- [35] Orović, J., Mrzljak, V., Poljak, I.: *Efficiency and Losses Analysis of Steam Air Heater from Marine Steam Propulsion Plant*, *Energies* 2018, 11, 3019 <https://doi.org/10.3390/en11113019>
- [36] Taner, T., Sivrioglu, M.: *Energy-exergy analysis and optimisation of a model sugar factory in Turkey*, *Energy*, 93, p. 641–654, 2015. <https://doi.org/10.1016/j.energy.2015.09.007>
- [37] Elsafi, A. M.: *Exergy and exergoeconomic analysis of sustainable direct steam generation solar power plants*, *Energy Conversion and Management* 103, p. 338–347, 2015. <https://doi.org/10.1016/j.enconman.2015.06.066>
- [38] Ameri, M., Ahmadi, P., Hamidi, A.: *Energy, exergy and exergoeconomic analysis of a steam power plant: A case study*, *International Journal of Energy Research* 33, p. 499–512, 2009. <https://doi.org/10.1002/er.1495>
- [39] *Marine Steam Turbine MS40-2 - Instruction Book For Marine Turbine Unit*, HYUNDAI-MITSUBISHI, HYUNDAI HEAVY INDUSTRIES CO., LTD., ULSAN, KOREA, 2004., internal ship documentation
- [40] Mrzljak, V., Senčić, T., Žarković, B.: *Turbogenerator Steam Turbine Variation in Developed Power: Analysis of Exergy Efficiency and Exergy Destruction Change*, *Modelling and Simulation in Engineering* 2018. <https://doi.org/10.1155/2018/2945325>
- [41] Cangiolli, F., Chatterton, S., Pennacchi, P., Netti, L., Ciuchicchi, L.: *Thermo-elasto bulk-flow model for labyrinth seals in steam turbines*, *Tribology International* 119, p. 359–371, 2018. <https://doi.org/10.1016/j.triboint.2017.11.016>
- [42] Lemmon, E. W., Huber, M. L., McLinden, M. O.: *NIST Reference Fluid Thermodynamic and Transport Properties-REFPROP*, Version 9.0, User's Guide, Colorado, 2010.
- [43] <http://www.krtproduct.com> (accessed: 09.01.2018)
- [44] <http://www.industriascontrolpro.com> (accessed: 09.01.2018)
- [45] <https://www.greisinger.de> (accessed: 05.01.2018)
- [46] <https://www.kyma.no> (accessed: 05.01.2018)
- [47] Mitrović, D., Živković, D., Laković, M. S.: *Energy and Exergy Analysis of a 348.5 MW Steam Power Plant*, *Energy Sources, Part A*, 32, p. 1016–1027, 2010. <https://doi.org/10.1080/15567030903097012>
- [48] Adibhatla, S., Kaushik, S. C.: *Energy and exergy analysis of a super critical thermal power plant at various load conditions under constant and pure sliding pressure operation*, *Applied Thermal Engineering*, 73, p. 51–65, 2014. <https://doi.org/10.1016/j.applthermaleng.2014.07.030>

- [49] Tadashi, T.: *Advances in Steam Turbines for Modern Power Plants*, Woodhead Publishing, Elsevier Ltd., 2017.
- [50] Baran, J.: *Redesign of steam turbine rotor blades and rotor packages – Environmental analysis within systematic eco-design approach*, Energy Conversion and Management 116, p. 18–31, 2016. <https://doi.org/10.1016/j.enconman.2016.02.067>
- [51] Kaushik, S. C., Reddy, V. S., Tyagi, S. K.: *Energy and exergy analyses of thermal power plants: A review*, Renewable and Sustainable Energy Reviews 15, p. 1857–1872, 2011. <https://doi.org/10.1016/j.rser.2010.12.007>
- [52] Aljundi, I. H.: *Energy and exergy analysis of a steam power plant in Jordan*, Applied Thermal Engineering 29, p. 324–328, 2009. <https://doi.org/10.1016/j.applthermaleng.2008.02.029>
- [53] Kopac, M., Hilalci, A.: *Effect of ambient temperature on the efficiency of the regenerative and reheat Catalagzi power plant in Turkey*, Applied Thermal Engineering 27, p. 1377–1385, 2007. <https://doi.org/10.1016/j.applthermaleng.2006.10.029>

Submitted: 26.01.2018. Vedran Mrzljak, [vedran.mrzljak@riteh.hr](mailto:vedran.mrzljak@riteh.hr)  
Faculty of Engineering, University of Rijeka, Vukovarska 58, 51000 Rijeka, Croatia

Accepted: 15.01.2019. Igor Poljak, [ipoljak2@unizd.hr](mailto:ipoljak2@unizd.hr)  
Department of maritime sciences, University of Zadar, Mihovila Pavlinovića 1,  
23000 Zadar, Croatia

Jasna Prpić-Oršić, [jasna.prpic-orsic@riteh.hr](mailto:jasna.prpic-orsic@riteh.hr)  
Faculty of Engineering, University of Rijeka, Vukovarska 58, 51000 Rijeka, Croatia